Journal of Magnetism and Magnetic Materials 351 (2014) 104–108

Contents lists available at ScienceDirect

Journal of Magnetism and Magnetic Materials

journal homepage: www.elsevier.com/locate/jmmm

Magnetic anisotropy in Fe films deposited on SiO_2/Si(001) and Si(001) substrates

S.V. Komogortsev [a,b,*], S.N. Varnakov [a,c], S.A. Satsuk [a], I.A. Yakovlev [a], S.G. Ovchinnikov [a,c,d]

[a] Kirensky Institute of Physics SB RAS, Akademgorodok, Krasnoyarsk 660036, Russia
[b] Siberian State Technological University, 82 Mira pr., Krasnoyarsk 660000, Russia
[c] Siberian State Aerospace University, 31 pr. im. gazety Krasnoyarskii rabochii, Krasnoyarsk 660014, Russia
[d] Siberian Federal University, 79 Svobodny Prospect, Krasnoyarsk 660041, Russia

ARTICLE INFO

Article history:
Received 8 June 2013
Received in revised form
23 September 2013
Available online 4 October 2013

Keywords:
Iron
Thin film
Magnetic anisotropy
Epitaxial growth

ABSTRACT

The magnetic anisotropy of 10 nm iron films deposited in an ultra high vacuum on the Si(001) surface and on the Si(001) over caped by 1.5 nm layer of SiO_2 was investigated. There is in-plane uniaxial magnetic anisotropy caused by oblique sputtering in the Fe films on a SiO_2 buffer layer. The easy magnetization axis is always normal to the atomic flux direction but the value of the anisotropy field is different depending on the axial angle among sputtering direction and the substrate crystallographic axes. It is argued that the uniaxial magnetic anisotropy results from elongated surface roughness formation during film deposition. Several easy magnetization axes are found in Fe/Si(001) film without the SiO_2 buffer layer. The mutual orientation of the main easy axes and Si crystallographic axes indicates that there is epitaxial growth of Fe/Si(001) film with the following orientation relative to the substrate: Fe[100] ∥Si[110]. The anisotropy energy of Fe/Si(001) film is estimated by simulation of angle dependence of remnant magnetization m_r as the sum of the m_r angle plot from uniaxial anisotropy (induced by oblique deposition) and the polar plot from biaxial magnetocrystalline anisotropy.

1. Introduction

Iron is a dominant material for thin magnetic films because of highest saturation magnetization (1700 G) and high Curie temperature (1044 K). To correct interpretation of the physical properties in iron ultra thin film (with a thickness less than 10 nm) it should be considered as a united system of film and substrate. Both the lattice mismatch at the film–substrate interface and the difference in electronic properties of them should be taken into account. The epitaxial Fe/Si [1–3] and Fe/SiO_2/Si [4–6] thin films attract researchers because of their interesting properties and prospects for spintronic devices. For example the current channels switching, which implies new applications in spintronics and can be controlled by the magnetic field, is revealed recently in such structures [5]. The investigation of magnetic anisotropy in iron films is important because the magnetization curve is governed by magnetic anisotropy. The easy magnetization plane, which coincides with the substrate surface, is a common and natural feature of thin magnetic films that originates from magnetic shape anisotropy [7,8]. The uniaxial magnetic anisotropy in the film plane is rather typical in the deposited films [7–10]. It may originate from anisotropic surface roughness formed due to oblique sputtering as well as by another structural and morphological features, and therefore it is sensitive to the sample preparation technique. This uniaxial magnetic anisotropy is important in different applications [11,12]. There can be a number of easy magnetization axes in the plane of thin epitaxial film deposited on the surface of a single crystal because of the ordered crystalline islands formation. The observation of such magnetocrystalline anisotropy can be useful as an indicator of epitaxial growth [12,13]. The experimental value of magnetocrystalline anisotropy energy is also of interest. It is established that in the films deposited on monocrystalline substrates the magnetic anisotropy energy depends on the angle among the flux direction and the crystallographic substrate axis [12,14,15], but there is no literature data about the SiO_2 spaser effect on magnetic anisotropy energy.

In this paper macroscopic magnetic anisotropy in the plane of iron films oblique sputtered on the (001) surface of single crystalline silicon is studied. Both the films deposited on the Si(001) surface and on the Si(001) over caped by 1.5 nm layer of SiO_2 were investigated.

2. Experimental

The iron films were deposited by thermal evaporation from Knudsen cells (boron nitride) in the ultrahigh-vacuum (UHV) modernized molecular-beam epitaxy (MBE) “Angara” setup [16]

* Corresponding author at: Kirensky Institute of Physics SB RAS, Akademgorodok, Krasnoyarsk 660036, Russia.
E-mail address: komogor_sergey@mail.ru (S.V. Komogortsev).

0304-8853/$ - see front matter © 2013 Elsevier B.V. All rights reserved.
http://dx.doi.org/10.1016/j.jmmm.2013.09.058

at room temperature (RT). The basic pressure in the growth chamber was 2.1×10^{-7} Pa. The evaporation process was controlled with a computer system, which included a hardware–software complex for the operation of the UHV. The thickness of the Fe films was controlled in situ by high-speed laser ellipsometry LEF-751 M [17]. Additional measurements of the Fe layer thickness were carried out ex situ by the X-ray fluorescence analysis. The growth rate of Fe films was about 0.25 nm/min. The effective thickness of iron films was 10 ± 1 nm. Both the crystallographic substrate orientation and the processes of cleaning and deposition were controlled by the high-energy electron diffraction (RHEED). The polished wafers of monocrystalline silicon Si(001) were used as substrates. The substrate was chemically cleaned with 1.5 nm thick SiO_2 protective layer formation on its surface [18,19]. This layer prevents mutual diffusion of the film and the substrate components [20]. To obtain the atomically pure surface of silicon the SiO_2 buffer layer was removed by heating at 900 °C. The procedure was carried out to the moment when the Si (001) 2×1 RHEED pattern was revealed.

The main axes which determine the film formation during deposition are the azimuthal sputtering direction and the crystallographic axes in the Si(001) plane (Fig. 1). The angle between the crucible axis and the normal to the substrate plane was 37° and the distance between the crucible outlet and the substrate center was 180 mm. Thus, the properties of the deposited iron films would depend on the value of the azimuthal angle between the crystallographic axis and the sputtering direction (Fig. 1). In this work the angle between the Si[110] direction and the sputtering axis is the azimuthal angle ϕ.

Four Fe/SiO_2/Si films with various values of the azimuthal angle ϕ were deposited. The symbols (A1–A4) marking the samples and used in the following are given in Table 1. Also, the film (marked further as B) was deposited on the Si(001) surface without the SiO_2 buffer layer.

Hysteresis loops were measured with a ferrometer adapted for magnetostatic properties study of thin magnetic films [21]. A uniform magnetic field (300 Oe, 50 Hz) generated with Helmholtz coils was applied parallel to the substrate plane. The film under study was located on the rotating plate between Helmholtz coils above the measuring coils. The magnetic circuit was locking in such a case and the electromotive force measured with the ferrometer is proportional to the magnetic moment projection to the applied field direction. To avoid the sample shape effect the circle samples with 14 mm in diameter which is equal to the distance between the measuring coils were chemically etched.

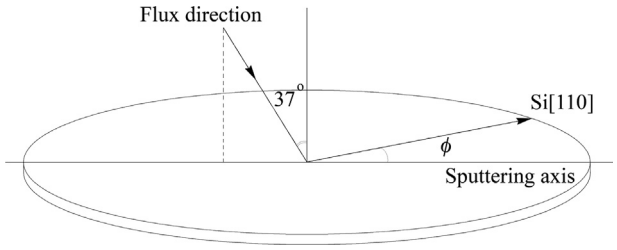

Fig. 1. Orientation of the Si substrate and the Fe atoms flux. The sputtering axis is turned on the azimuthal angle ϕ relative to Si[110] direction in the Si(001) plane.

Table 1
The magnetic anisotropy field of Fe/SiO_2/Si(001) and Fe/Si(001) films.

Sample	A1	A2	A3	A4	B
Azimuthal angle ϕ (°)	105	0	15	45	40
$H_a(Oe)$	160 ± 10	100 ± 10	150 ± 20	50 ± 5	115 ± 5

3. Results and discussion

3.1. Magnetic anisotropy of Fe/SiO_2/Si(001) films

There is in-plane uniaxial magnetic anisotropy in the Fe films deposited on SiO_2/Si(001) as one can see from the angular dependence of the hysteresis loop shape and the normalized remanent magnetization value $m_r = M_r/M_s$ (Fig. 2). The M_s value used to calculate m_r was taken equal to the magnetization at $H = 300$ Oe. The easy magnetization axis is perpendicular to the atomic flux direction. Such orientation of easy magnetization axis was observed for the films deposited by oblique sputtering [12,22–26]. Angular dependencies of the hysteresis loop shape are similar for all four samples deposited on SiO_2. Therefore, only the A1 sample dependence will be discussed further (Fig. 2, Table 1).

The hysteresis loop is rectangular in the easiest magnetization direction, hence the remanent magnetization value here is $m_r = 1$. If the film magnetization follows the uniform rotation, then the m_r value will be the residual magnetization projection to the applied field direction given by $m_r = \cos(\eta)$ and $\eta = \theta + \pi/2$, where η is the angle between the applied field direction and the easy magnetization axis and θ is the angle between the applied field direction and the sputtering axis. Such dependence is consistent with the measured values of m_r (Fig. 2). Thus, the studied films are remagnetized by the uniform rotation. This result is expected for the films with a uniform thickness of about 10 nm [9,27]. The value of the uniaxial magnetic anisotropy field H_a can be estimated from the saturation field $H_s = H_a$ measured in the applied field along the hard magnetization axis. The H_a values measured in this way are given in Table 1.

The anisotropy field H_a is different for the samples A1, A2, A3, A4 deposited at different values of azimuthal angle ϕ. The deposition conditions of the A1 and A3 samples can be considered as equivalent. The angle $\phi = 105°$ (A1) between the sputtering axis and the Si[110] direction corresponds to the angle $\phi = 15°$

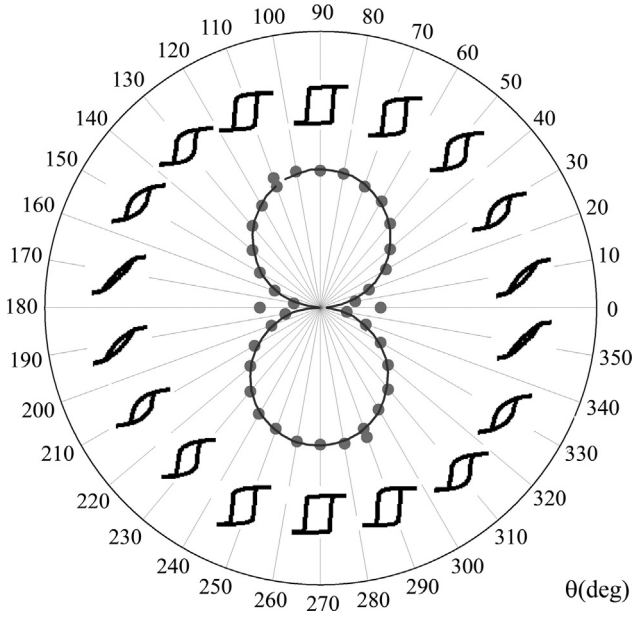

Fig. 2. The hysteresis loop shape and remanent magnetization value (filled symbols) in the Fe film deposited on SiO_2/Si(001) (sample A1) with $\phi = 105°$ measured at different applied field directions. The θ is the angle between the applied field direction and the sputtering axis. The solid line is $m_{r\_uniaxial} = \cos(\theta + \pi/2)$.

between the sputtering axis and the Si[−110] direction (A3), because both Si[110] and Si[−110] crystallographic directions are absolutely equivalent in single-crystalline silicon. Therefore it is not surprised that A1 and A3 films are characterized by the identical H_a values. The anisotropy field in the A2 sample ($\phi = 0^\circ$) is slightly lower than that in the A1 and A3 samples and the H_a field in the A4 sample deposited with the sputtering axis oriented along Si[100] ($\phi = 45^\circ$) is even less. Thus, it can be argued that in the iron film deposited on the SiO_2 buffer layer the sputtering axis direction relative to the Si[110] axis does not affect the orientation of easy magnetization axis and the symmetry of magnetic anisotropy, but it affects the magnetic anisotropy field value. The uniaxial magnetic anisotropy in the oblique sputtered films is attributed to the self-shadowing effects [12,23,28], anisotropic strain at the interface [28–30], etc. Activity in this area has been in progress for several decades, but the model explaining the easy magnetization axis perpendicular to the deposition direction in the oblique sputtered films by a steering effect has been developed quite recently [22,23]. This steering effect results from the distortion of sputtered atom trajectories due to the long-range attractive forces between the incident atoms and the atoms of substrate [22,23]. The steering effect results in the formation and subsequent growth of anisotropic surface roughness that elongated perpendicular to the sputtering direction [22–24,26,31]. Finally the uniaxial magnetic anisotropy is originated from the anisotropic surface relief.

The elongated surface roughness is observed by atomic force microscope (AFM) imaging of the Fe films deposited on SiO_2/Si (001) (Fig. 3a). According to Schlömann [32], the magnetic anisotropy field caused by the anisotropic surface relief in the film can be estimated as

$$H_{as} \approx M_s 4\pi^2 p^2/(\lambda d), \quad (1)$$

where M_s is a saturation magnetization, p is the random mean square (RMS) deviation from the average flat level surface, λ is the prevalent wavelength in surface roughness, d is the film thickness.

From the fast Fourier transform (FFT) analysis of the AFM image (see Fig. 3b) the prevalent wavelength is $\lambda = 0.4 \pm 0.1$ μm and the RMS deviation of thickness is $p = 3.0 \pm 0.5$ nm. Using the determined values of λ, p and $M_s = 1700$ G for bulk bcc-Fe and $d = 10$ nm the estimation is found to be $H_{as} \approx 80$–270 Oe. The estimated value of the magnetic anisotropy field H_{as} from the anisotropic surface relief is close to the values of magnetic anisotropy field H_a presented in Table 1. This confirms that the in-plane magnetic anisotropy of the Fe films deposited on SiO_2/Si (001) is arisen from the anisotropic surface roughness formation during sputtering.

The magnetic anisotropy of Fe film deposited on the clean Si (001) surface (the sample B) is qualitatively different from one of the Fe films deposited on the SiO_2/Si(001) surface (Fig. 4). There are two axes of easy magnetization in the $m_r(\theta)$ plot (Fig. 4), which are along the segments connecting the maxima in the $m_r(\theta)$ plot. These axes are found to be parallel to the Si[110] and Si[−110] axes of the silicon substrate. In addition, the polar plot in Fig. 4 is somewhat elongated in the direction perpendicular to the sputtering axis and slightly sheared relative to this direction. The 10 nm thick Fe films under study have a body-centered cubic (bcc) structure [33]. The most perfect lattice match of bcc-Fe and Si (001) surface needs parallel orientation of Fe(001) and Si(001) planes [34]. Such epitaxial growth of bcc-Fe on the Si(001) surface would result in two easy magnetization axes in the film plane, which coincide with the crystallographic directions bcc-Fe[100] and [010] (Fig. 5). The conclusion from data and examination of Figs. 4 and 5 is: the Fe film (sample B) is epitaxially grown on the Si(001) surface so that bcc-Fe[100] ∥ Si[110]. The established bcc-Fe[100] ∥ Si[110] lattice matching is consistent with the crystallographic criterion – the axes with the maximum density of atomic

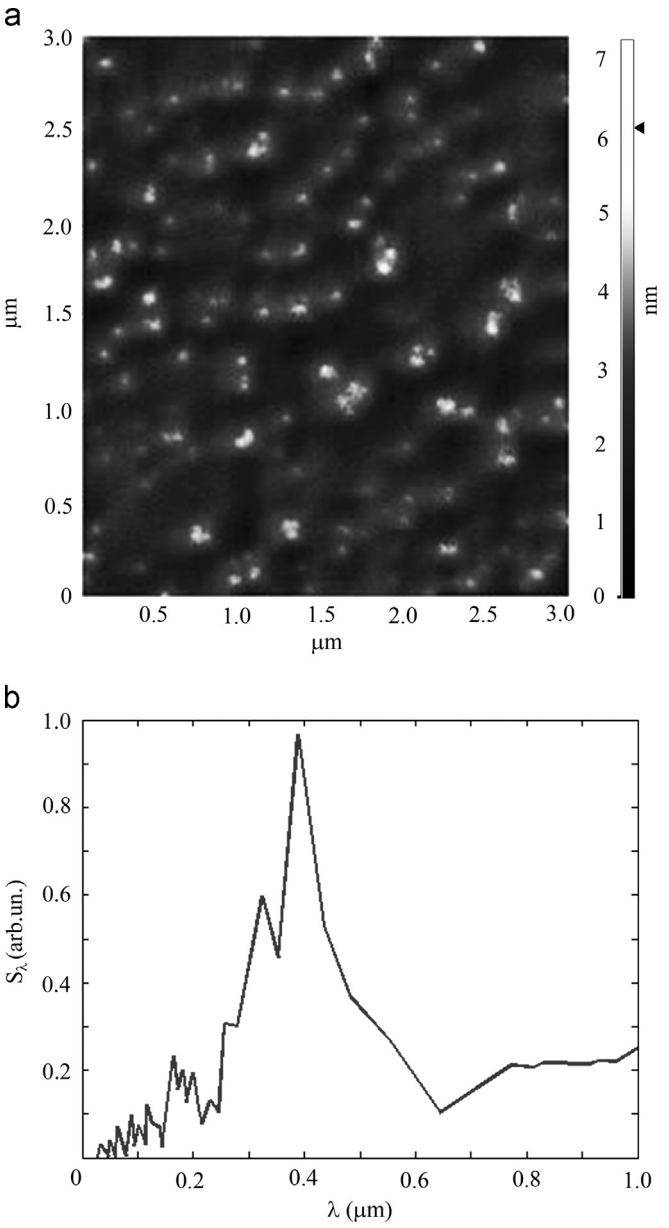

Fig. 3. (a) The AFM image of the Fe film deposited on SiO_2/Si(001). (b) The FFT spectrum of the AFM image along the axis perpendicular to the long axis of anisotropic roughness.

packing are parallel in two most perfectly matching lattices [35]. The elongation of the $m_r(\theta)$ plot in Fig. 4 is supposed to be due to the uniaxial magnetic anisotropy formation in the process of oblique sputtering. The observed little shear of the $m_r(\theta)$ plot in Fig. 4 is also expected since the easy magnetization axis deviates from crystallographic substrate direction by 5° (see Table 1). The above conclusions were used for the quantitative description of the $m_r(\theta)$ plot (Fig. 4). The uniform rotation of the magnetization results in the following expression for the $m_r(\theta)$ dependence in the bcc-Fe film due to magnetocrystalline anisotropy solely:

$$m_{r\_cubic} = m_{max} \cos \xi,$$
$$-\pi/4 < \xi < \pi/4 \quad \text{or } 3/4 < \xi < 5\pi/4 \quad (2)$$

and

$$m_{r\_cubic} = m_{max} \sin \xi,$$
$$\pi/4 < \xi < 3\pi/4 \text{ or } 5\pi/4 < \xi < 7\pi/4, \quad (3)$$

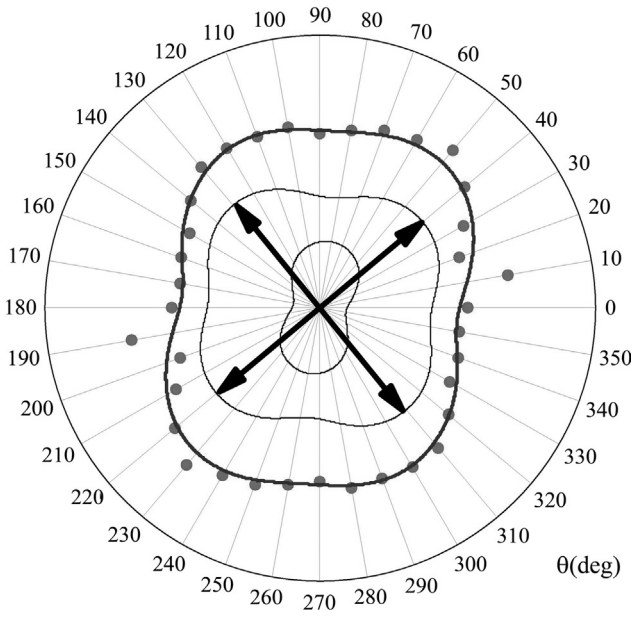

Fig. 4. The remanent magnetization (filled circles) in the Fe film deposited on the clean (001)Si surface (the sample B) measured at different applied field directions. θ is the angle between the applied field direction and the sputtering axis. The bold arrows indicate the [110]Si and [−110]Si axes. The bold line is the plot of expression $m_r(\theta)=(1-x)m_{r\_cubic}(\theta+\phi)+xm_{r\_uniaxial}(\theta)$. The thin lines show the contributions from uniaxial and biaxial anisotropies.

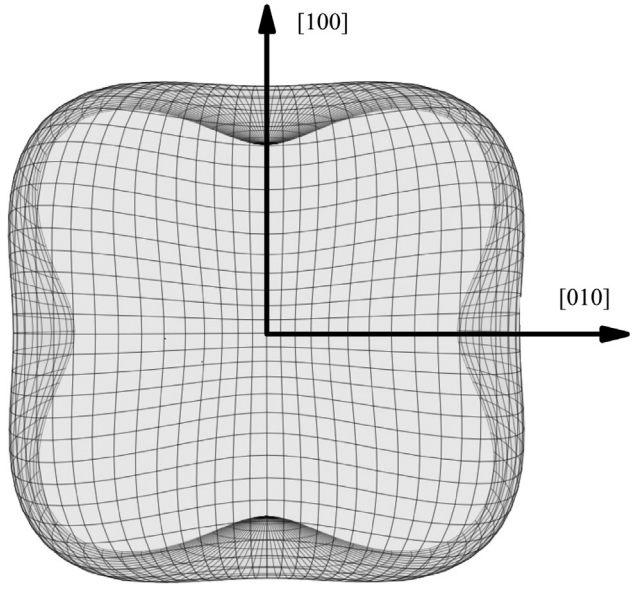

Fig. 5. The cross-section of the magnetocrystalline anisotropy energy surface in bcc-Fe by the Fe(001) plane parallel to the Si(001) plane. The arrows indicate easy magnetization axes along the both [100] and [010] bcc-Fe crystallographic axes.

where ξ is the angle between the applied field and the bcc-Fe [100] axis.

Since the uniaxial anisotropy from the oblique sputtering $m_{r\_uniaxial}(\eta)=\sin(\eta)$, where η is the angle between the applied field direction and the easy magnetization axis, would contribute in total $m_r(\theta)$ dependence also, the resulting $m_r(\theta)$ dependence is

$$m_r(\theta)=(1-x)m_{r\_cubic}(\theta+\phi)+xm_{r\_uniaxial}(\theta+\phi 1), \quad (4)$$

where x is the contribution of uniaxial anisotropy to the total magnetic anisotropy energy of the film, ϕ is the angle between the easy magnetization axis of bcc-Fe and the sputtering axis, $\phi 1$ is the angle between the easy magnetization axis induced by oblique sputtering and the sputtering axis, θ is the angle between the applied field direction and the sputtering axis.

The possible dispersion in orientation of various epitaxial bcc-Fe islands and the dispersion of the elongated roughness directions on the surface were taken into account in the final simulated $m_r(\theta)$ dependence in Fig. 4. The averaging by ϕ and $\phi 1$ was made with Gaussian distribution function. The final simulated $m_r(\theta)$ plot corresponding to the best fitting of experimental $m_r(\theta)$ data for the Fe film deposited on the Si(001) surface (the sample B) is in Fig. 4. The best fit is approached at $x = 0.35$.

Assuming that the uniaxial anisotropy constant induced by oblique sputtering is the same as for the A4 sample we found the magnetocrystalline anisotropy constant $K_{uniaxial}=4.3\times10^4$ erg/cm^3 (calculated as $K_{uniaxial}=H_aM_s/2$, where H_a is taken from Table 1), and using the obtained $x = 0.35$, it is possible to estimate the magnetocrystalline anisotropy constant for the epitaxial Fe film (the sample B) as $K_{cubic}=K_{uniaxial}(1-x)/x$ [36–38]. The result of the estimation is $K_{cubic}=7.9\times10^4$ erg/cm^3. This value of K_{cubic} is much lower than the magnetocrystalline anisotropy constant of bulk bcc-Fe $K_{Fe}=4.8\times10^5$ erg/cm^3. Such a magnetocrystalline anisotropy constant decrease can be understood as a result of the penetration of silicon atoms from the Si substrate into the Fe film. Such a penetration occurs during the Fe film deposition on the Si and resulted in the bcc-Fe solid solution formation [3,20,33,39]. Indeed, the magnetocrystalline anisotropy constant of the bcc-Fe solid solution containing 7.5 wt.% of Si is $K_{cubic}\approx10\times10^4$ erg/cm^3 [40] which is close to the estimated K_{cubic} value.

4. Conclusions

Magnetic anisotropy of the 10 nm thick Fe films deposited in the ultrahigh vacuum on the crystalline silicon surface Si(001), and Si(001) surface covered with a thin SiO_2 buffer layer was investigated. The in-plane uniaxial magnetic anisotropy was found in the films deposited on the SiO_2 layer. The easy magnetization axis in these films is perpendicular to the atom flux direction. The anisotropy field is different for various orientations of the deposition axis relative to the crystallographic axis of the Si substrate. It is argued that this magnetic anisotropy was due to the elongated roughnesses of the film surface formed in an oblique sputtering process. The films deposited on the clean Si(001) surface have a two easy magnetization axes indicating the epitaxial growth of Fe film on Si. The magneto-crystalline anisotropy constant of Fe/Si (001) epitaxial film was estimated by simulating the angular dependence of remanent magnetization. The magneto-crystalline anisotropy constant of the epitaxial Fe film is close to the solid solution constant of the Fe containing 7.5 wt.% of Si.

Acknowledgments

The work has been supported by RFBR Grant 11-03-00168-a, 12-02-00943-a, 13-02-01265-a, Interdisciplinary integration of fundamental research of SB RAS (2012-2014) project No. 64. Also the study was supported by The Ministry of Education and Science of Russian Federation, project 14.513.11.0016.

References

[1] S.A. Wolf, D.D. Awschalom, R.A. Buhrman, J.M. Daughton, S.V. Molnar, M.L. Roukes, A.Y. Chtchelkanova, D.M. Treger, Science 294 (2001) 1488.
[2] S. Datta, B. Das, Applied Physics Letters 56 (1990) 665.
[3] R.R. Gareev, D.E. Bürgler, M. Buchmeier, R. Schreiber, P. Gareev, Journal of Magnetism and Magnetic Materials 240 (2002) 235.

[4] V.V. Balashev, V.V. Korobtsov, T.A. Pisarenko, E.A. Chusovitin, Physics of the Solid State 51 (3) (2009) 601.
[5] N.V. Volkov, E.V. Eremin, A.S. Tarasov, et al., Journal of Magnetism and Magnetic Materials 324 (2012) 3579.
[6] N.V. Volkov, A.S. Tarasov, E.V. Eremin, A.V. Eremin, S.N. Varnakov, S.G. Ovchinnikov, Journal of Applied Physics 112 (2012) 123906.
[7] J.M.D. Coey, Magnetism and Magnetic Materials, Cambridge University Press, 2009.
[8] R.C.O. Handley, Modern Magnetic Materials: Principles and Applications, John Wiley & Sons, New York, 1972.
[9] M. Prutton, Thin Ferromagnetic Films, London Butterworths, 1964.
[10] Nguyen N. Phuoc, Feng Xu, C.K. Ong, Journal of Applied Physics 105 (2009) 113926.
[11] Xiaoqiang Zhu, Zhenkun Wang, Yi Zhang, Li Xi, Jianbo Wangn, Qingfang Liu, Journal of Magnetism and Magnetic Materials 324 (2012) 2899.
[12] Qing-feng Zhan, Chris Van Haesendonck, Stijn Vandezande, Kristiaan Temst, Applied Physics Letters 94 (2009) 042504.
[13] K.S. Ermakov, Yu.P. Ivanov, L.A. Chebotkevich, Physics of the Solid State 52 (12) (2010) 2555.
[14] J.L. Bubendorff, S. Zabrocki, G. Garreau, S. Hajjar, R. Jaafar, D. Berling, A. Mehdaoui, C. Pirri, G. Gewinner, Europhysics Letters 75 (1) (2006) 119.
[15] S. Yunsic, V. Borovikov, J.G. Amar, Physical Review B 77 (2008) 235423.
[16] S.N. Varnakov, A.A. Lepeshev, S.G. Ovchinnikov, A.S. Parshin, M.M. Korshunov, P. Nevoral, Instruments and Experimental Techniques 47 (6) (2004) 839.
[17] E.V. Spesivtsev, S.V. Rihlitskii, V.A. Shvets, Patent 2302623, Russian Federation, Ellipsometer, No. 19 (10.07.2007).
[18] A. Ishizaka, Y. Shiraki, Journal of The Electrochemical Society: Electrochemical Science and Technology (1986) 666.
[19] N.V. Volkov, A.S. Tarasov, E.V. Eremin, S.N. Varnakov, S.G. Ovchinnikov, S.M. Zharkov, Journal of Applied Physics 109 (2011) 123924.
[20] S.N. Varnakov, S.V. Komogortsev, S.G. Ovchinnikov, J. Bartolome, J. Sese, Journal of Applied Physics 104 (9) (2008) 094703.
[21] Grinin, L.V. Sokolenko, V.A. Frolov, A.P. Feoktistov, Ustroistvo dla opredelenia magnitnih harakteristik ferromagnitnih materialov, Patent No. 1112328, USSR (08.05.1984).
[22] Sebastiaan van Dijken, Giovanni Di Santo, Bene Poelsema, Physical Review B 63 (2001) 104431.
[23] Sebastiaan van Dijken, Giovanni Di Santo, Bene Poelsema, Applied Physics Letters 77 (2000) 2030.
[24] G. Garreau, J.L. Bubendorff, S. Hajjar, D. Berling, S. Zabroki, A. Mehdaoui, R. Stephan, P. Wetzel, G. Gewinner, C. Pirri, Physica Status Solidi (c) 1 (12) (2004) 3726.
[25] J.H. Wolfe, R.K. Kawakami, W.L. Ling, Z.Q. Qiu, R. Arias, D.L. Mills, Journal of Magnetism and Magnetic Materials 232 (2001) 36.
[26] Chiao-Sung Chi, Bo-Yao Wang, Way-Faung Pong, Tsung-Ying Ho, Cheng-Jui Tsai, Fang-Yuh Lo, Ming-Yau Chern, Wen-Chin Lin, Journal of Applied Physics 111 (2012) 123918.
[27] E.M. Bradly, M. Prutton, Journal of Electronics and Control 6 (1959) 81.
[28] S. Smith, Anisotropy in permalloy films, Journal of Applied Physics 30 (1959) 264.
[29] D.S. Chuang, C.A. Ballentine, R.C.O. Handley, Physical Review B 49 (1994) 15084.
[30] P. Krams, B. Hillebrands, G. Guntherodt, H.P. Oepen, Physical Review B 49 (1994) 3633.
[31] Z.Y. Park, E. Fullerton, S.D. Bader, Applied Physics Letters 66 (1995) 2140.
[32] Ernst Schlömann, Journal of Applied Physics 41 (1970) 1617.
[33] S.N. Varnakov, S.G. Ovchinnikov, J. Bartolome, J. Rubin, L. Badia, G.V. Bondarenko, Solid State Phenomena 168–169 (2011) 277.
[34] V.M. Ievlev, Structural Transformation in Thin Films, Metallurgia, Moscow, 1988.
[35] Palatnik, I.I. Papirov, The Oriented Crystallization, Metallurgia, Moscow, 1964.
[36] J. Geshev, M. Mikhov, J.E. Schmidt, Journal of Applied Physics 85 (1999) 7321.
[37] S.I. Smirnov, S.V. Komogortsev, Journal of Magnetism and Magnetic Materials 320 (2008) 1123.
[38] N.A. Usov, J.M. Barandiaran, Journal of Applied Physics 112 (2012) 053915.
[39] S.N. Varnakov, J. Bartolome, J. Sese, S.G. Ovchinnikov, S.V. Komogortsev, A.S. Parshin, G.V. Bondarenko, Physics of the Solid State 49 (8) (2007) 1470.
[40] L.P. Tarasov, Physical Review B 56 (1939) 1231.